

# RSC Advances



This is an *Accepted Manuscript*, which has been through the Royal Society of Chemistry peer review process and has been accepted for publication.

*Accepted Manuscripts* are published online shortly after acceptance, before technical editing, formatting and proof reading. Using this free service, authors can make their results available to the community, in citable form, before we publish the edited article. This *Accepted Manuscript* will be replaced by the edited, formatted and paginated article as soon as this is available.

You can find more information about *Accepted Manuscripts* in the [Information for Authors](#).

Please note that technical editing may introduce minor changes to the text and/or graphics, which may alter content. The journal's standard [Terms & Conditions](#) and the [Ethical guidelines](#) still apply. In no event shall the Royal Society of Chemistry be held responsible for any errors or omissions in this *Accepted Manuscript* or any consequences arising from the use of any information it contains.

## Eggshell/Fe<sub>3</sub>O<sub>4</sub> nanocomposite: A novel magnetic nanoparticles coated on porous ceramic eggshell waste as an efficient catalyst in the synthesis of 1,8-dioxo-octahydroxanthene

Received 00th January 20xx,  
Accepted 00th January 20xx

DOI: 10.1039/x0xx00000x

www.rsc.org/

Elaheh Mosaddegh,<sup>\*a</sup> Fatemeh Alsadat Hosseininasab,<sup>b</sup> and Asadollah Hassankhani<sup>a</sup>

Eggshell/Fe<sub>3</sub>O<sub>4</sub> nanocomposite was simply synthesized via an economic and novel method using an aqueous solution of FeSO<sub>4</sub> as a starting material and recycled eggshell biowaste as coating agent without any additional alkali and protection atmosphere. Furthermore, the catalytic activity of the magnetic nanocomposite was investigated in the synthesis of 1,8-dioxo-octahydroxanthenes under solvent-free conditions. The reaction proceeds to completion in short reaction time with excellent yield. The suggested strategy for synthesizing 1,8-dioxo-octahydroxanthenes is of great interest because a novel, green, and low-cost magnetic nanocomposite is used as a heterogeneous catalyst, on account of its convenient preparation and high reusability.

### Introduction

Natural products with a xanthene heterocyclic motif such as 9-aryl-1,8-dioxo-octahydroxanthenes show a broad spectrum of important biological and pharmaceutical in the field of medicinal chemistry which include antibacterial, antiviral, anti-inflammatory agents, anticancer activities [1-3] and novel CCR1 receptor antagonists [4] as well as their efficiency in the field of material science as dyes [5], laser technologies for visualization of biomolecules, fluorescent markers [6] and luminescent sensors [7]. In this regards, there are several reports on their synthesis in the presence of different catalyst [8-19]. However, the reported methods suffer from drawbacks such as long reaction times, moderate yields, the use of toxic and expensive catalysts and reagents with high catalyst loading, and no agreement with the aspect of green chemistry. Thus, the value of a green and the high effective protocol for this important class of heterocycles depends mainly on identifying a simple, cheap, highly effective and green catalyst [13].

Iron oxide nanoparticles such as magnetite (Fe<sub>3</sub>O<sub>4</sub>) have attracted considerable attention in recent years due to their potential applications in magnetic media, catalysis, color imaging, ferrofluids, and biomedicine [20-22]. The most popular methods for preparation of magnetic nano particles (MNPs) are thermal decomposition [23–25] and coprecipitation [26–28]. In the coprecipitation method, Fe<sub>3</sub>O<sub>4</sub> nanoparticles are prepared from a mixture of Fe<sup>2+</sup> and Fe<sup>3+</sup> salt solutions by adding an alkali under

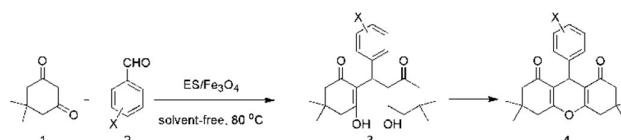
protective atmosphere [26–28]. Since nanoparticles synthesized by coprecipitation method have attend to be polydisperse in size, the addition of an inorganic coating agent with high thermal stability [29] can be enhanced stability of MNPs [30, 31].

Eggshell (ES) wastes are abundant and inexpensive biomaterials which are composed of more than 90% calcium carbonate [32,33]. ES shows high thermal stability, relatively lower density and phase continuity in the composite compared to mineral CaCO<sub>3</sub> [34]. In addition, the porous structure of ES makes it to use less material to form higher surface area compared to artificial one [35]. In this regards, the porous structure of the ES with wide nucleation sites to minimize the aggregation of particles is an excellent host for supporting MNPs. So, in this work, a new and highly effective strategy is used for the synthesis of novel ES/Fe<sub>3</sub>O<sub>4</sub> nanocomposite by using ES bioceramic for coating MNPs via co-precipitation method. To our knowledge, this is the first report to green synthesis of MNPs supported on ES waste as a natural and biocompatible composite. In addition, the catalytic activity of the nanocomposite was investigated in the synthesis of 1,8-dioxo-octahydroxanthenes via one pot multi-component condensation of aryl aldehydes and dimedone in solvent-free and thermal conditions (Scheme 1).

### Results and Discussions

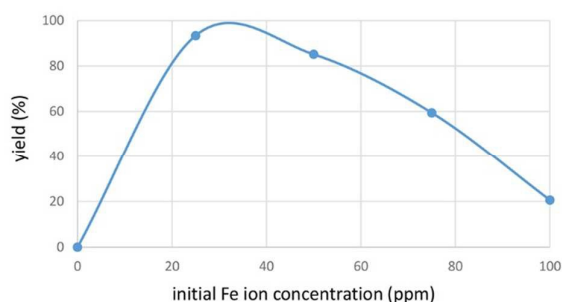
#### Characterization of ES/Fe<sub>3</sub>O<sub>4</sub> nanocomposite

In order to investigate the highest MNPs deposition on the ES surface, different concentrations of Fe<sup>2+</sup> ion solution were treated

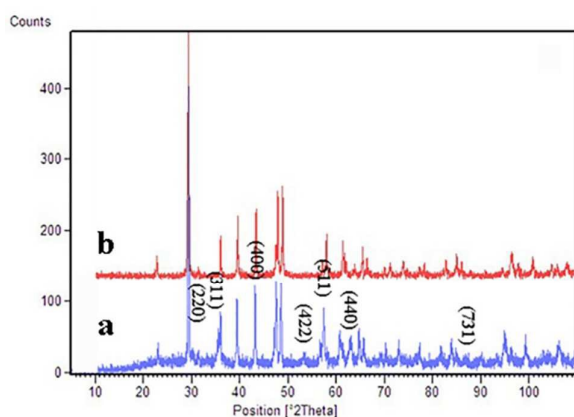


<sup>a</sup> Department of New Materials, Institute of Science and High Technology and Environmental Sciences, Graduate University of Advanced Technology, PO Box 76315-117, Kerman, Iran.

<sup>b</sup> Department of Chemistry, Faculty of Science, Hormozgan University, PO Box 3995, Bandarabbas, Iran.

**Scheme 1** Synthesis of 1,8-dioxo-octahydroxanthenes, biowaste derivatives

catalyzed by ES/Fe<sub>3</sub>O<sub>4</sub> nanocomposite.

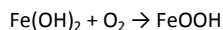
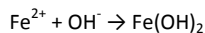
**Fig. 1** Adsorption of Fe ion on the eggshell support.**Fig. 2** XRD pattern of a) magnetic ES/Fe<sub>3</sub>O<sub>4</sub> nanocomposite and b) raw eggshell.

with the ES powder in the same condition as mentioned in the experimental section. As shown in Fig. 1, the highest recovery of the metal ion was observed at a concentration of 1000 mg L<sup>-1</sup>. It was proven the recovery decreases at higher concentrations, but the amount of adsorbed metal ions increases due to the higher initial metal ion concentration. Therefore, the concentration of 1000 mg L<sup>-1</sup> was used as the maximum concentration of the initial ion solution in the synthesis of the nanocomposite. Furthermore, the structure and chemical composition of the synthesized composite with an optimized amount of Fe ions were fully characterized.

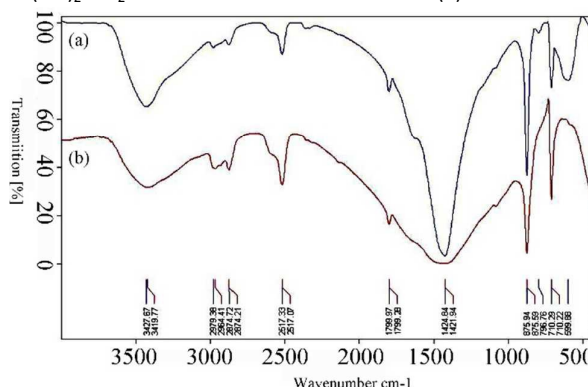
### XRD analysis

The eggshell has a basic nature which can provide an alkaline media with pH of 9.5 by forming Ca(OH)<sub>2</sub> in its surface structure. Therefore, ES acts as alkali as well as coating agent to precipitate Fe<sup>2+</sup> without any use of more external base and protective atmosphere. According to Eq. 1, Fe(OH)<sub>2</sub> was oxidized by O<sub>2</sub> in air to form FeOOH. Combination of Fe(OH)<sub>2</sub> and FeOOH at 60 °C was produced Fe<sub>3</sub>O<sub>4</sub> particles [37-38] which grew on the porous surface of ES. It indicated that the use of ES support can produce Fe<sub>3</sub>O<sub>4</sub> with no need to involve Fe<sup>3+</sup> as precursors. The phase composition of the

nanocomposite can be deduced from the XRD pattern (Fig. 2) with those of known literature [40].



(1)

**Fig. 3** FTIR spectra of a) ES/Fe<sub>3</sub>O<sub>4</sub> nanocomposite and b) raw ES.

It can be seen from the XRD patterns that the main peak at  $2\theta=29.4$  is related to the major phase of CaCO<sub>3</sub> in eggshell structure [41] and the peaks at (220), (311), (400), (422), (511), (440) and (731) are relevant to the phase of Fe<sub>3</sub>O<sub>4</sub> [42]. All diffraction peaks arising from the structure of the nanocomposite are similar to those reported in the literature [40,41]. Further, the presence of iron was approved with energy dispersion x-ray (EDX) analysis of nanocomposite that showed high levels of Fe (38.1%), Ca (27.0%), O (24.9%) and carbon (9.4%) with small amounts of P (0.2%), Zn (0.2) and Na (0.2%). The XRD investigation revealed that the as-synthesized magnetic Fe<sub>3</sub>O<sub>4</sub> and ES NPs have average diameters of 13 and 18 nm respectively as calculated with the Scherrer equation ( $D = \frac{K\lambda}{\beta \cos\theta}$ ).

### FTIR spectra analysis

Comparing the FTIR spectra of ES/Fe<sub>3</sub>O<sub>4</sub> MNPs and eggshell (Fig. 3) shows the typical carbonate absorptions at about 2517 (HCO<sub>3</sub>), 1799 (CO), 1424, 710 (C–O) and 876 cm<sup>-1</sup> (OCO) which are according to the literature [42]. The broad band at about 3427 cm<sup>-1</sup> is due to OH stretching vibration in Ca(OH)<sub>2</sub> formed during adsorption of water on the surface of the composite structure. Furthermore, the strong FTIR band observed at around 599 cm<sup>-1</sup> can be attributed to the Fe-O-Fe stretching vibration mode of Fe<sub>3</sub>O<sub>4</sub> [43].

### Thermo Gravimetric Analysis (TGA)

The thermal stability of the catalyst was investigated by the thermal gravimetric analysis (TGA) and compared with raw ES (Fig. 4). The differential scanning calorimetry (DSC) and TGA analysis which performed from room temperature to 900 °C indicated that the main weight loss in both raw ES (Fig. 4b) and the ES/Fe<sub>3</sub>O<sub>4</sub> composite (Fig. 4a) is related to the decomposition of ES to CO<sub>2</sub> and CaO that proves the existence of the carbonate in the eggshell structure [40]. The measured weight loss below 600°C is due to

release of physically adsorbed water [36]. So, the catalyst remained stable in the reaction temperature (80 °C).

structure of eggshell with spherical morphology provides a large contact area for catalyzing the reaction.

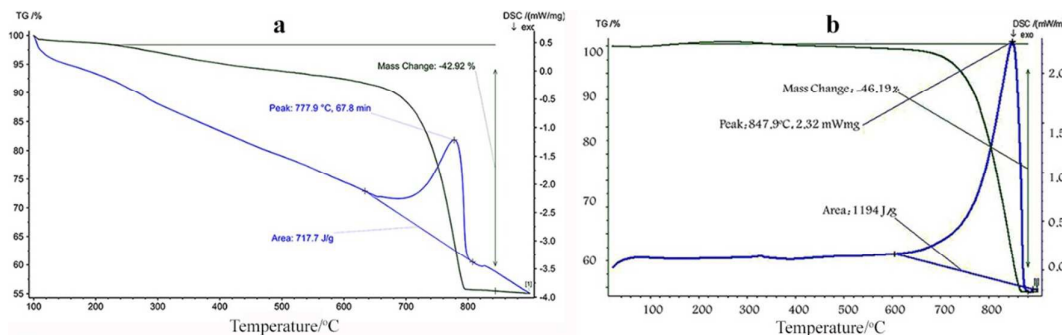


Fig. 4 TGA curve of (a) ES/Fe<sub>3</sub>O<sub>4</sub> MNPs and (b) raw ES.

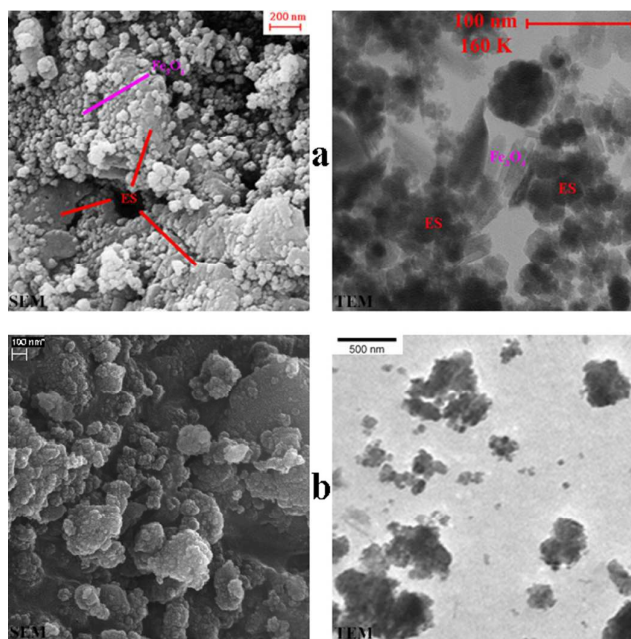


Fig. 5 TEM and FESEM images of (a) ES/Fe<sub>3</sub>O<sub>4</sub> nanocomposite and (b) raw ES.

#### Electron microscopic investigation

Transmission microscopy (TEM) and field emission scanning electron microscopy (FESEM) of eggshell supported magnetic nanoparticles and raw eggshell have provided in Fig. 5a and b respectively. It is verifying from the comparison of TEM of raw eggshell with the supported one that the Fe<sub>3</sub>O<sub>4</sub> MNPs were coated on the surface of the ES as nanoribbon structure. The TEM investigation also showed the average diameter of 13 nm for the magnetic Fe<sub>3</sub>O<sub>4</sub> nanoribbon which is in good agreement with the data arising from Scherrer equation. Furthermore, FESEM image showed well dispersion capability of the ES/Fe<sub>3</sub>O<sub>4</sub> nanocomposite, which should be due to decreasing of electrostatic force and high surface energy of the magnetic particles after coating with ES. In general, the great dispersion of Fe<sub>3</sub>O<sub>4</sub> nanoribbons on the porous

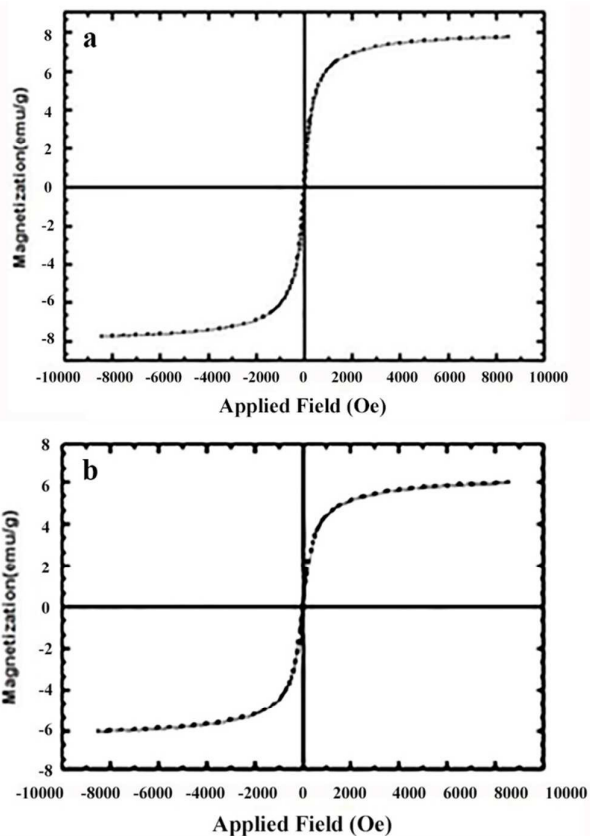


Fig. 6 VSM plot of a) magnetic nanocomposite and b) pure Fe<sub>3</sub>O<sub>4</sub>.

#### VSM analysis

VSM plot of ES/Fe<sub>3</sub>O<sub>4</sub> magnetic nanocomposite was shown in Figure 6. The symmetric hysteresis displays magnetic behaviors of the composite. This is because that the diameter of as-synthesized magnetic nanocomposite (18 nm) is smaller than that of critical threshold of Fe<sub>3</sub>O<sub>4</sub> (25 nm) [43]. As shown in Fig. 6a and b, the saturation magnetization of magnetic nanocomposite is smaller

than that of pure  $\text{Fe}_3\text{O}_4$ . This small saturation magnetization ( $7.68 \text{ emu}\cdot\text{g}^{-1}$ ) may attribute to the small particle size effect of magnetic nanocomposite since a noncollinear spin arrangement occurs primarily at or near the surface [43]. This phenomena result in the reduction of the magnetic moment in magnetic nano particles [44].

**Table 1** Synthesis of 3,3,6,6-tetramethyl-9-(4-nitro-phenyl)-1,8-dioxo-1,2,3,4,5,6,7,8-octahydroxanthene in the presence of different catalyst.

Entry	Catalyst	Time	Yield (%) <sup>a</sup>
1	ES/ $\text{Fe}_3\text{O}_4$	15 min	95
2	ES	2 h	93
3	ES+ $\text{Fe}_3\text{O}_4$	2 h	86
4	$\text{Fe}_3\text{O}_4$	2 h	82
5	$\text{CaCO}_3/\text{Fe}_3\text{O}_4$	2 h	74

<sup>a</sup>Yield refers to isolated pure product.

**Table 2** Nano ES/ $\text{Fe}_3\text{O}_4$ -catalyzed synthesis of 3,3,6,6-tetramethyl-9-phenyl-1,8-dioxo-1,2,3,4,5,6,7,8-octahydroxanthene derivatives.

Entry	Ar	Yield (%) <sup>a</sup>	m.p. (°C) <sup>[ref]</sup>
1	$\text{C}_6\text{H}_5$	92	199–201 <sup>[8]</sup>
2	4-Cl- $\text{C}_6\text{H}_4$	93	233–235 <sup>[8]</sup>
3	3- $\text{NO}_2$ - $\text{C}_6\text{H}_4$	95	168–170 <sup>[8]</sup>
4	2,4- $\text{Cl}_2$ - $\text{C}_6\text{H}_4$	97	247–249 <sup>[8]</sup>
5	4-Br- $\text{C}_6\text{H}_4$	98	244–246 <sup>[58]</sup>
6	2-OH- $\text{C}_6\text{H}_4$	90	182–184 <sup>[58]</sup>
7	4-OH- $\text{C}_6\text{H}_4$	98	246–248 <sup>[8]</sup>
8	4- $\text{CH}_3\text{O}$ - $\text{C}_6\text{H}_4$	96	241–243 <sup>[8]</sup>
9	4- $\text{NO}_2$ - $\text{C}_6\text{H}_4$	95	222–224 <sup>[8]</sup>
10	4-( $\text{CH}_3$ ) <sub>2</sub> N- $\text{C}_6\text{H}_4$	94	219–221 <sup>[8]</sup>

<sup>a</sup>Yield refers to isolated pure product.

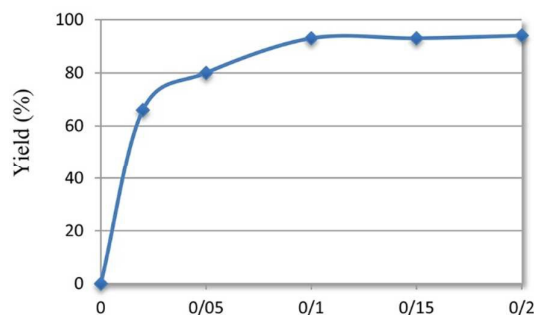
### Synthesis of 1,8-dioxo-1,2,3,4,5,6,7,8-octahydroxanthene derivatives

The activity of the nanocatalyst was tested using a one-pot three-component condensation of dimedone (2 eq) with different aromatic aldehydes (1 eq) under solvent-free and thermal conditions to obtain the corresponding 1,8-dioxo-octahydroxanthenes. Our attempts to synthesis of compound 4 in the absence of the catalyst produced only compound 3 and no cyclization product was obtained even after 5 h (Scheme 1). Next, the optimum amount of nanocatalyst was evaluated in the range of 0.02–0.2 g as summarized in Fig 7. The optimum amount of catalyst was 0.1 g. Further increasing the amount of catalyst did not show significant improvement on the yield or reaction time.

In order to investigate the role of  $\text{Fe}_3\text{O}_4$  MNPs in enhancing the catalytic activity of the ES, we decided to carry out comparative reactions in the presence of the ES/ $\text{Fe}_3\text{O}_4$ , raw ES, pure  $\text{Fe}_3\text{O}_4$  and physically mixed ES and  $\text{Fe}_3\text{O}_4$  (Table 1). As described in table 2 (entries 1–3), the raw ES is the best catalyst after ES/ $\text{Fe}_3\text{O}_4$  nanocomposite and the physically mixed ES- $\text{Fe}_3\text{O}_4$  could not be improved its catalytic activity (entry 3), whereas, the chemical

mixture of ES and  $\text{Fe}_3\text{O}_4$  could improve the catalytic activity of the ES effectively.

Since almost 90% of the eggshell is composed calcium carbonate and it is the main active site of eggshell catalyst, we carried out a

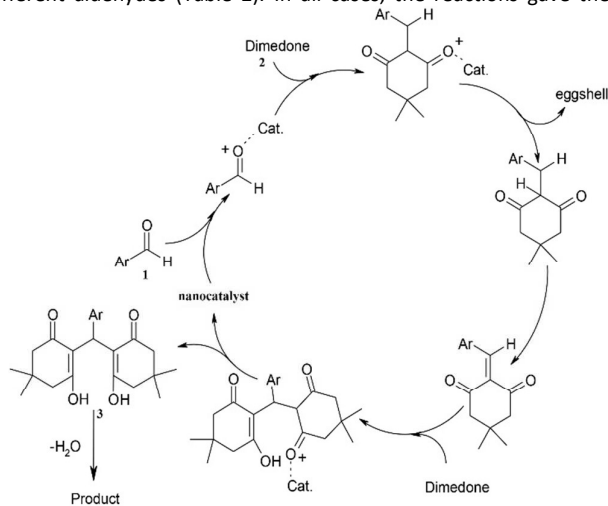


comparative reaction in the presence of  $\text{CaCO}_3/\text{Fe}_3\text{O}_4$  (0.1 g) in the

**Fig. 7** Optimization of catalyst amount.

**Scheme 2** Plausible mechanistic pathway for the synthesis of 1,8-dioxo-1,2,3,4,5,6,7,8-octahydroxanthene derivatives.

same conditions. Compared with the nanocomposite, the reaction time was too longer and the product yield was low. This proves that eggshell has high porosity with much higher surface area naturally. In summary, the ES/ $\text{Fe}_3\text{O}_4$  nanocomposite showed a higher yield in very short reaction time in comparison with the other catalyst. Therefore, the role of the ES/ $\text{Fe}_3\text{O}_4$  system as a multifunctional bio-derived catalyst with improved catalytic activity was proven. Furthermore, the generality of this reaction was examined using different aldehydes (Table 2). In all cases, the reactions gave the



corresponding products in excellent yields (90–98%) and in very short reaction times (15 min). This method offers significant improvements with regard to the scope of the transformation, simplicity, and green aspects by avoiding expensive, hazardous or corrosive catalysts.

A possible mechanism for the formation of the products is shown in Scheme 2. In this reaction, intermediate 3 was formed through Knoevenagel reaction between dimedone and aldehyde, and

subsequently, elimination of water was occurred from the intermediate **3** to give compound **4**.

Eco-friendly conditions, ease of separation, stability and reusability of the heterogeneous catalysts are of the most important benefits and make them useful for green commercial and industrial

applications. The reusability of the nanocatalyst was examined in the synthesis of 1,8-dioxo-octahydroxanthenes (Table 2, entry 2).

The catalyst was recovered magnetically after each run, washed three times with hot EtOH, dried in an oven at 120 °C, and tested for

**Table 3** A comparison of various methods in the synthesis of  $\text{Ca}_2\text{Fe}_2\text{O}_5$  phase.

Entry	Catalyst	Reaction conditions	Time/Yield (%)	Reference
1	Amberlyst-15	Catalyst amount: 200 mg $\text{CH}_3\text{CN}$ (10 mL), Reflux	5 h/94	45
2	p-dodecylbenzenesulfonic acid	Catalyst amount: 10 mol% $\text{H}_2\text{O}$ (20 mL), ultrasonic irradiation	1 h/94	10
3	$\text{NaHSO}_4 \cdot \text{SiO}_2$	Catalyst amount: 100 mg $\text{CH}_3\text{CN}$ (10 mL), Reflux	6.5 h/93	46
4	silica chloride	Catalyst amount: 100 mg $\text{CH}_3\text{CN}$ (10 mL), Reflux	6 h/90	46
5	1-Methylimidazolium trifluoroacetate: [Hmim]TFA	Catalyst amount: 100 mg 80 °C	3.5 h/82	47
6	Alum	Catalyst amount: 10 mol% $\text{H}_2\text{O}$ (10 mL), 80 °C	25 min/94	48
7	$\text{SmCl}_3$	Catalyst amount: 20 mol% solvent-free, 120 °C	8 h/97	50
8	Cellulose sulfonic acid	solvent-free, 110 °C	5 h/95	51
9	[Bmim]HSO <sub>4</sub>	solvent-free, 80 °C	1.5/85	52
10	[Bmim]ClO <sub>4</sub>	Catalyst amount: 4 mmol 100 °C	1 h/94	53
11	Sulfamic acid	Catalyst amount: 10 mol% solvent-free, heat	11 h/94	54
12	LiBr	Catalyst amount: 15 mol% solvent-free, heat	1 h/84	55
13	Tetrabutylammonium hydrogen sulfate	Catalyst amount: 10 mol% Aqueous 1,4-dioxane (20 mL), reflux	3 h/94	56
14	Tetrabutylammonium Bromide	Catalyst amount: 40 mol% solvent-free, 120 °C	5 h/97	56
15	$\text{InCl}_3 \cdot 4\text{H}_2\text{O}$	Catalyst amount: 22 mg 80 °C	40 min/96	57
16	Nano $\text{Fe}_3\text{O}_4$	Catalyst amount: 10 mol% solvent-free, 100 °C	15 min/90	58
17	$\text{ZrOCl}_2 \cdot 8\text{H}_2\text{O}$	Catalyst amount: 12 mg solvent-free, 80 °C	25 min/95	59
18	ES/ $\text{Fe}_3\text{O}_4$	Catalyst amount: 100 mg solvent-free, 80 °C	15 min/95	Present work

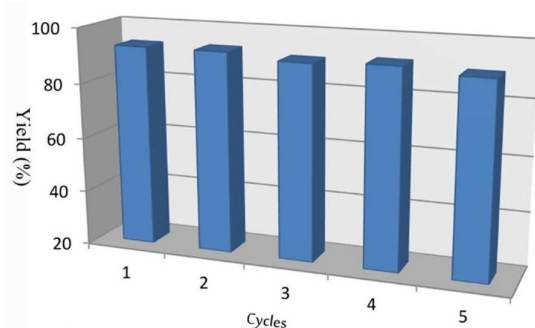


**Fig. 8** Recycling experiment of nanocatalyst.

its activity in subsequent runs (Fig. 8). It was found that the catalyst could be reused five times without any loss of activity. Thus, the new procedure is green, cost effective, clean and more efficient

than reported methods with ease of separation of the catalyst from the reaction mixture. This claim is justified through representative examples from more recently published literature with conventional catalyst, illustrated in Table 3.

## Experimental Section

### Materials and Instrument

All chemicals used in this work, were of analytical reagent grade, purchased from Merck. IR spectra were obtained with MATSON1000 FT-IR spectrophotometer. X-ray diffraction (XRD) with an X-Pert Philips PW340/60 diffractometer (40kV and 30mA) and  $\text{Cu K}\alpha$  radiation ( $\lambda=0.154$  nm) was used to analyze the structure of the composite. TGA experiments were

carried out using an STA 409 PC Luxx thermal analysis machine (NETZSCH, Germany) under a flow of nitrogen. The morphology of the cross section of the film was examined with a scanning electron microscope (SEM) (Seron Tech. AIS 2100) and transition electron microscopy (TEM) (Philips, CM 120). The magnetic property of MNPs was measured using an Alternating Gradient Force Magnetometer (AGFM, Iran).

#### General procedure for the preparation of magnetic ES/Fe<sub>3</sub>O<sub>4</sub> nanocomposite

The eggshell powder was prepared according to our previous method [36]. Following, 1.0 g of the ES powder mixed simplicity with 50.0 mL of FeSO<sub>4</sub> solution in the concentration of 25-1000 mgL<sup>-1</sup>. The suspension was stirred vigorously in a baker at 60 °C. The black ES/Fe<sub>3</sub>O<sub>4</sub> nano-composite was produced after 2 h. The resulted particles were magnetically separated and washed with deionized water three times to remove any excess salts from the suspension. The products were then dried at 60 °C for further characterizations.

#### General procedure for the preparation of 1,8-dioxo-octahydroxanthenes

In a typical general procedure, a mixture of 4-chlorobenzaldehyde (0.14 g, 1 mmol) and dimedone (0.28 g, 2 mmol) in solvent-free condition at 80 °C, were stirred thoroughly in the presence of a catalytic amount of catalyst (0.1 g) to afford the corresponding 1,8-dioxo-octahydroxanthenes in excellent yields. After completion of the reaction (TLC), hot EtOH was added to the reaction mixture and stirred for 5 min. Then the solid catalyst was magnetically separated from the soluble products and washed with hot EtOH. After cooling, the crude products were precipitated. Pure 1,8-dioxo-octahydroxanthenes were obtained in high yields without any use of more purification. All compounds were known in the literature [8-19] and the NMR and IR spectra of the products were in agreement with earlier data [8-19]. The selected spectral data of four representative 1,8-dioxo-1,2,3,4,5,6,7,8-octahydroxanthenes are given in supplementary information.

#### Conclusions

In summary, an efficient, green, and alkali-free synthesis of magnetic ES/Fe<sub>3</sub>O<sub>4</sub> nanocomposite has been established without any protective atmosphere by simply heterogeneous stirring FeSO<sub>4</sub> aqueous solution with eggshell powder as coating agent via a thermal co-precipitation method. The Fe<sub>3</sub>O<sub>4</sub> NPs showed magnetic properties even after coating. Moreover, a green, rapid and highly efficient protocol for the one-pot synthesis of 1,8-dioxo-octahydroxanthenes has been described under thermal and solvent-free conditions using ES/Fe<sub>3</sub>O<sub>4</sub> nanocomposite as a heterogeneous and green catalyst with high catalytic activity and reusability. Finally, the synthesis of nanocomposite based on porous ceramic ES waste is interesting because of the potential to lower cost design new materials in various fields especially in organic transformation and reducing environmental problems.

#### Acknowledgements

The financial support of the Graduate University of Advanced Technology is gratefully acknowledged (project 7/4736).

#### Notes and references

- R. D. Jonathan, K. R. Srinivas and E. B. Glen, *Eur. J. Med. Chem.* 1988, **23**, 111.
- J. Robak and R. J. Gryglewski, *Pol. J. Pharmacol.* 1996, **48**, 555; H. K. Wang, S. L. Lee and K. H. Morris-Natschke, *Med. Res. Rev.* 1997, **17**, 367; V. Rukavishnikov, M. P. Smith, G. B. Birrell, J. F. W. Keana and O. H. Griffith, *Tetrahedron Lett.* 1998, **39**, 6637.
- N. Mulakayala, P. V. N. S. Murthy, D. Rambabu, M. Aeluri, R. Adepu, G. R. Krishna, C. M. Reddy, K. R. S. Prasad, M. Chaitanya, C. S. Kumar, M. V. B. Rao and M. Pal, *Bioorg. Med. Chem. Lett.* 2012, **22**, 2186.
- A. Naya, M. Ishikawa, K. Matsuda, K. Ohwaki, T. Saeki, K. Noguchi and N. Ohtake, *Bioorg. Med. Chem. Lett.* 2003, **11**, 875; Wang H, Lu L, Zhu S, Li Y and Cai W. *Curr. Microbiol.* 2006, **52**, 1.
- P. Srihari, S. S. Mandal, J. S. S. Reddy, R. Srinivasa Rao and J. S. Yadav, *Chin. Chem. Lett.* 2008, **19**, 771.
- G. Pohlars, J. C. Scaiano and R. F. Sinta, *Chem. Mater.* 1997, **9**, 3222; C. G. Knight and T. Stephens, *Biochem. J.* 1989, **258**, 683.
- J. F. Callan, A. P. de Silva and D. C. Magri, *Tetrahedron* 2005, **61**, 8551; O. Sirkecioglu, N. Talinli and A. Akar, *J. Chem. Res. (S)* 1995, 502; A. Banerjee and A. K. Mukherjee, *Stain. Technol.* 1981, **56**, 83; J. P. Poupelin, G. Saint-Rut and O. J. Foussard-Blanpin, *Med. Chem.* 1978, **13**, 67.
- T. S. Jin, J. S. Zhang, J. C. Xiao, A. Q. Wang and T. S. Li, *Synlett* 2004, 866.
- F. Darvish, S. Balalaei, F. Chadegani and P. Salehi, *Synth. Commun.* 2007, **37**, 1059.
- T. S. Jin, J. S. Zhang, A. Q. Wang and T. S. Li, *Ultrason. Sonochem.* 2006, **13**, 220.
- S. Rostamizadeh, A. M. Amani, G. H. Mahdavinia, G. Amiri and H. Sepehrian, *Ultrason. Sonochem.* 2010, **17**, 306.
- N. Mulakayala, G. P. Kumar, D. Rambabu, M. Aeluri, M. V. B. Rao and M. Pal, *Tetrahedron Lett.* 2012, **53**, 6923.
- A. Ilangovan, S. Muralidharan, P. Sakthivel, S. Malayappasamy, S. Karuppusamy and M. P. Kaushik, *Tetrahedron Lett.* 2013, **54**, 491.
- M. Seyyedhamzeh, P. Mirzaei and A. Bazgir, *Dyes Pigm.* 2008, **76**, 836.
- E. Mosaddegh, M. R. Islami and A. Hassankhani, *Arab. J. Chem.* 2012, **5**, 77.
- A. Hasaninejad, M. Dadar and A. Zare, *Chem. Sci. Trans.* 2012, **1**, 233.
- F. Shirini, M. Abedini and R. Pourhasan *Dyes Pigm.* 2013, **99**, 250.
- F. Shirini and N. Ghaffari Khaligh, *Dyes Pigm.* 2012, **95**, 789.
- B. Hamers, E. Kosciusko-Morizet, C. Müller, and D. Vogt, *ChemCatChem.* 2009, **1**, 103.
- L. Shen, P. E. Laibinis and T. A. Hatton, *Langmuir* 1999, **15**, 447.
- J. Q. Cao, Y. X. Wang, J. F. Yu, J. Y. Xia, C. F. Zhang, D. Z. Yin and U. O. Hafeli, *J. Magn. Magn. Mater.* 2004, **277**, 165.
- Q. Li, Y. M. Xuan and J. Wang, *Exp. Therm. Fluid Sci.* 2005, **30**, 109.
- J. Park, K. An, Y. Hwang, J. G. Park, H. J. Noh, J. Y. Kim, J. H. Park, N. M. Hwang and T. Hyeong, *Nat. Mater.* 2004, **3**, 891.
- F. X. Redl, C. T. Black, G. C. Papaefthymiou, R. L. Sandstorm, M. Yin, H. Zeng, C. B. Murray and S. P. O'Brien, *J. Am. Chem. Soc.* 2004, **126**, 14583.
- S. Sun, H. Zeng, D. B. Robinson, S. Raoux, P. M. Rice, S. X. Wang and G. Li, *J. Am. Chem. Soc.* 2004, **126**, 273.
- A. Bee, R. Massart and S. Neveu, *J. Magn. Magn. Mater.* 1995, **149**, 6.

- 27 J. P. Jolivet, C. Chaneac and E. Tronc, *Chem. Commun.* 2004, 481.
- 28 X. Wang, J. Zhuang, Q. Peng and Y. Li, *Nature* 2005, **437**, 121.
- 29 Y. Zhu, L. P. Stubbs, F. Ho, R. Liu, C. P. Ship, J. A. Maguire and N. S. Hosmane, *ChemCatChem* 2010, **2**, 365.
- 30 S. I. Stoeva, F. Huo, J. S. Lee and C. A. Mirkin, *J. Am. Chem. Soc.* 2005, **127**, 15362.
- 31 M. A. Correa-Duarte, M. Grzelczak, V. Salgueirino-Maceira, M. Giersig, L. M. Liz-Marzan, M. Farle, K. Sieradzki and R. Diaz, *J. Phys. Chem. B* 2005, **109**, 19060.
- 32 E. Mosaddegh and A. Hassankhani, *Chin. J. Catal.* 2014, **35**, 351.
- 33 G. Suresh Kumar, A. Thamizhave and E. K. Girija, *Mater. Lett.* 2012, **76**, 198.
- 34 P. S. Guru and S. Dash, *Adv. Colloid Interface Sci.* 2014, **209**, 49.
- 35 J. Z. Zhang, J. G. Wang and J. J. Ma, *J. Zhejiang Univ. SCI.* 2005, **6A**, 1095.
- 36 a) E. Mosaddegh and A. Hassankhani, *Catal. Commun.* 2013, **33**, 70; b) E. Mosaddegh, *Ultrason. Sonochem.* 2013, **20**, 1436.
- 37 P. Refait and J. M. R. Genin, *J. Mater. Res.* 1993, **34**, 797.
- 38 A. A. Olowe and J. M. R. Genin, *J. Mater. Res.* 1991, **32**, 965.
- 39 C. Hui, C. Shen, T. Yang, L. Bao, J. Tian, H. Ding, C. Li and H. J. J. Gao, *Phys. Chem. C* 2008, **112**, 11336.
- 40 S. Sheng-Nan, W. Chao, Z. Zan-Zan, H. Yang-Long, S. S. Venkatraman and X. Zhi-Chuan, *Chin. Phys. B* 2014, **23**, 037503.
- 41 Y. Wei, B. Han, X. Hu, Y. Lin, X. Wang and X. Deng, *Procedia Eng.* 2012, **27**, 632.
- 42 E. Mosaddegh, A. Hassankhani and H. Karimi-Maleh, *Mater. Sci. Eng. C* 2015, **46**, 264.
- 43 L. Levy, Y. Sahoo, K. Kim, E. J. Bergey and P. N. Prasad, *Chem. Mater.* 2002, **14**, 3715.
- 44 S. F. Si, C. H. Li, X. Wang, D. P. Yu, Q. Peng and Y. D. Li, *Cryst. Growth Des.* 2005, **5**, 391.
- 45 B. Das, P. Thirupathi, I. Mahender, V. S. Reddy and Y. K. Rao, *J. Mol. Catal. A: Chem.* 2006, **247**, 233.
- 46 B. Das, P. Thirupathi, K. R. Reddy, B. Ravikanth and L. Nagarapu, *Catal. Commun.* 2007, **8**, 535.
- 47 M. Dabiri, M. Baghbanzadeh and E. Arzroomchilar, *Catal. Commun.* 2008, **9**, 939.
- 48 B. R. Madje, M. B. Ubale, J. V. Bharad and M. S. Shingare, *S. Afr. J. Chem.* 2010, **63**, 36.
- 49 H. A. Soliman and T. A. Salama, *Chin. Chem. Lett.* 2013, **24**, 404.
- 50 A. Llangovan, S. Malayappasamy, S. Muralidharan and S. Maruthamuthu, *Chem. Cent. J.* 2011, **5**, 81.
- 51 H. A. Oskooie, L. Tahershamsi, M. M. Heravi and B. Baghernejad, *E-J. Chem.* 2010, **7**, 717.
- 52 K. Niknam and M. Damya, *J. Chin. Chem. Soc.* 2009, **56**, 659.
- 53 S. Makone and S. Mahurkar, *Green Sus. Chem.* 2013, **3**, 27.
- 54 A. Saini, S. Kumar and J.S. Sandhu, *Synlett* 2006, 1928.
- 55 B. Rajitha, B.S.Kumar and Y.T. Reddy, *Tetrahedron Lett* 2005, **46**, 8691.
- 56 H. N. Karade, M. Sathe, and M. P. Kaushik, *ARKIVOC* 2007 **xiii**, 252.
- 57 B. Karamia, S. Nejatib and K. Eskandari, *Curr. Chem. Lett.* 2015, **4**, 169.
- 58 M. A. Ghasemzadeh, A. Safaei-Ghomi and S. Zahedi, *J. Serb. Chem. Soc.* 2013, **78**, 769.
- 59 E. Mosaddegh, M. R. Islami and A. Hassankhani, *Arab. J. Chem.* 2012, **5**, 77.

## Graphical Abstract

